

# Thermoluminescence of Aluminium Nitride: Influence of the Thermal Treatment

F. Porte,<sup>a</sup> J. P. Lecompte,<sup>a</sup> J. Jarrige,<sup>a</sup> A. Collange,<sup>b</sup> P. Grosseau<sup>b</sup> and B. Guilhot<sup>b</sup>

<sup>a</sup>LMCTS ESA CNRS 6015–123, Avenue A. Thomas, 87060 Limoges Cedex, France

<sup>b</sup>SPIN-CRESA ENSMSE–158, Cours Fauriel, 42023 St Etienne Cedex 2, France

## Abstract

*Aluminium nitride powders are very sensitive to oxidation: nitrogen atoms are easily substituted by oxygen atoms in the hexagonal structure. Thermoluminescence (TL), in detecting defects in the matter can be used to study oxygen impurities in the AlN lattice. So we tested two powders with different synthesis processes and thermal treatments in order to observe the influence of the oxygen content on the TL curves. First aluminium nitride synthesised with amines and aluminium halides revealed the relation between the TL signal and crystallite size: the TL intensity increased despite the removal of oxide phases and the decrease of oxygen content. Second, Pyrofine R AlN was treated under oxygen flow for 3 h between 200° and 1100°C. The TL spectrum showed the presence of  $\gamma$ -AlON at low temperature and the area of the TL peak (80°C) increased with the weight ratio of AlN. Published by Elsevier Science Limited.*

## 1 INTRODUCTION

Aluminium nitride is a novel-based ceramic material. Its bondings is rather ionic-covalent (the rate of ionicity changes between 0.36 and 0.56), the result being several good properties of the dense material

It crystallises with the hexagonal würtzite structure<sup>1,2</sup> ( $a = 3.1105 \pm 0.0005$  Å and  $c = 4.9788 \pm 0.008$  Å) in which the spatial group is  $P6_3mc$ .<sup>3</sup> Each atom of aluminium takes up the centre of a tetrahedron composed of four nitrogen atoms.

Aluminium nitride has a large band GAP of 6.3 eV<sup>4</sup> that makes it a good insulating material. In addition, its high thermal conductivity ( $\lambda = 320 \text{ WmK}^{-1}$  for monocrystals,  $200 \text{ WmK}^{-1}$  for polycrystals sintered with yttria additives)<sup>5</sup> makes it useful in microelectronics as a substrate.

In contrast, aluminium nitride is very sensitive to water and oxygen: we observed the formation of aluminium hydroxide and ammonia.<sup>6,7</sup>

In fact, oxygen has a high affinity towards aluminium and an atomic radius smaller than nitrogen, so aluminium nitride has a high ability to accommodate large quantities of oxygen without phase separation. Then there is the formation of aluminium vacancies to conserve the electric charge of the matter<sup>8,9</sup>(Fig. 1).

Harris *et al.*<sup>10</sup> have argued that at first there is a decrease of the lattice parameter when the oxygen content improves, followed by an expansion of the cell volume: when the oxygen content achieves the critical concentration (0.75 at %), two type  $V_{Al} + O_N$  defects combine themselves to give a single octahedric defect and make two vacancies disappear. For example, 2 wt% of oxygen modifies the rate  $c/a$  from 1.633 to 1.572.<sup>11</sup> Furthermore, they suggest that there is a relation between the intensity of luminescence and the luminescence peak position, e.g. the oxygen content.

The luminescence of aluminium nitride with or without doping was often studied in the past. Authors<sup>12–15</sup> have analysed the system AlN:Mn and their findings indicate that the red or orange luminescence observed is connected with the  $Mn^{4+}$  ion in the AlN lattice and green luminescence with the  $Mn^{2+}$  ion. Thus, the light emission is related to transitions from the metastable levels to basic levels of the tetravalent or divalent manganese ion.

In the AlN:O crystals,<sup>16,17</sup> there occur several types of complex centres<sup>18–20</sup> which are formed by an aluminium vacancy and one or several oxygen atoms occupying various lattice sites around the vacancy. These centres are responsible for the observed signals in thermoluminescence.<sup>21</sup>

This paper presented thermal treatments undergone by AlN powders and their analysis by T.L with any attempt to link signal T.L and powder characteristics (XRD, ...) and finally to interpret

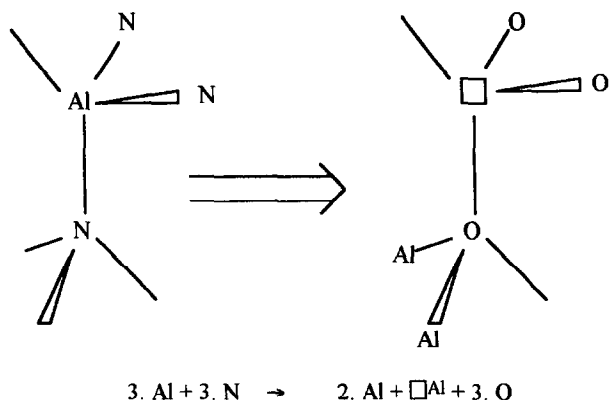


Fig. 1. Mechanism of nitrogen substitution by oxygen.

the results with mechanisms and models proposed by authors.

## 2 Materials and Experimental Procedure

### 2.1 Materials

The aluminium iodide produced by Cerac is pure at 99.9%. Propylamine comes from Aldrich: the purity is better than 99%. Three gases are used during experiments: ammonia (99.995% purity) from Union Carbide and nitrogen N (synthesis) and U (thermal treatment) from 'Air Products'. Products are used as received. In the second part, the AlN Pyrofine powder is prepared by Elf Atochem by a carbonituration process.

### 2.2 Synthesis and thermal treatments<sup>22</sup>

Experiments are conducted in an airtight assembly (Fig. 2) in a dynamic atmosphere. Reactions take place at 40°C (thermostatic bath) over a 24 h period: 500 mg of iodide are introduced into the quartz tube, then a primary vacuum is conducted for 1 h in order to remove gases in the assembly. With a system of depressure/superpressure between

Part D and Part G, propylamine is added in excess to the solid iodide.

The reaction is very exothermic and we observed the formation and expansion of a brownish precipitate. A low stream of nitrogen is maintained during the reaction. The propylamine left-over is removed by hot evaporation under vacuum. Components resulting from the reaction are pyrolysed under ammonia stream at 1100°C for 1 h with a rise of 5°C min<sup>-1</sup>. Some thermal treatments under nitrogen beyond 1100°C (rise: 5°C min<sup>-1</sup>, dwell time: 3 h) ended at crystallised powders.

### 2.3 Thermoluminescence : techniques and experimental conditions

#### 2.3.1. Theory

Thermoluminescence is a technique employed to detect defects in matter. The substitution of some atoms by impurities in the lattice implies the presence of some defects in the GAP. (Fig. 3(a)) An excitation by a UV lamp makes electrons and holes move from the valency band to the GAP: these are trapped by crystalline defects. (Fig. 3(b)) Electrons and holes trapped are removed by thermal activation, and recombinations of Donor-Acceptor complexes produce emissions of light due to numerous overlapping bands (Fig. 3(c)). Thus, an emission luminescence spectra is obtained (Fig. 3(d)).

#### 2.3.2. Operating method

The AlN powder was mixed with acetone (such as 1g d'AlN for 79.1g d'acetone). A small amount of the solution (~2 mg) was dropped on an copper cupel, then the acetone was allowed to evaporate.

The temperature was lowered at -196°C with liquid nitrogen followed by an excitation by a UV low-pressure mercury lamp, Mineralight model SCT-1, working at a wavelength of  $\lambda = 254 \text{ nm}$  (4.89 eV) for 2 min.

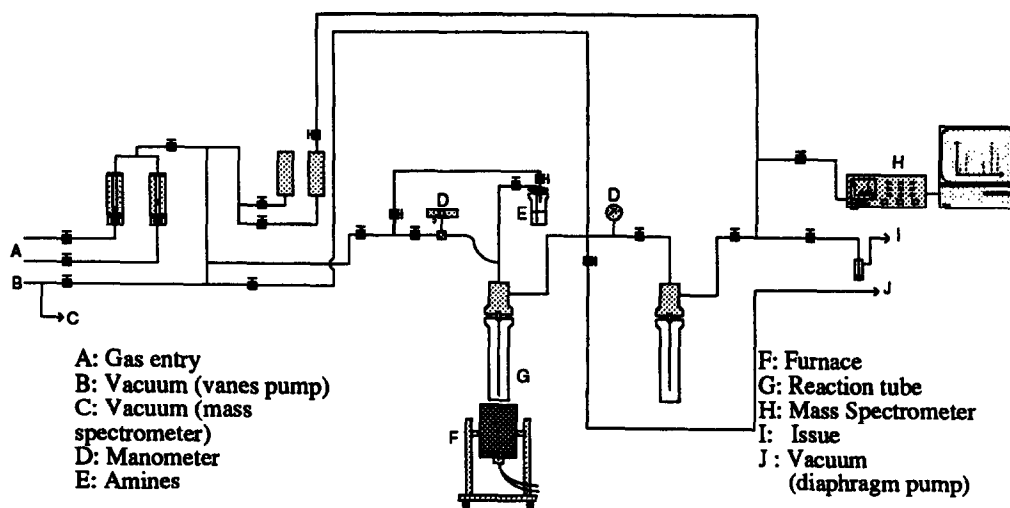


Fig. 2. Airtight assembly.

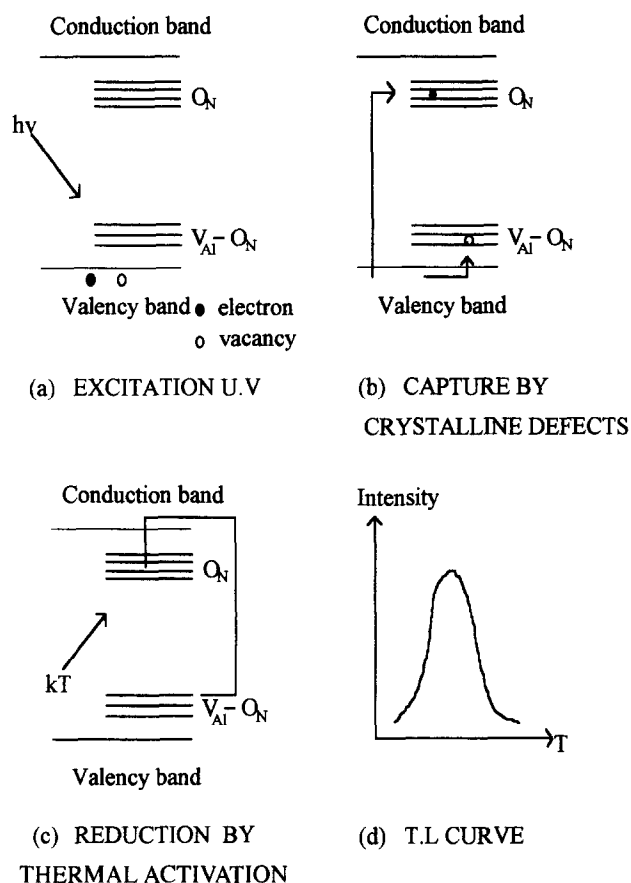


Fig. 3. Theory of thermoluminescence.

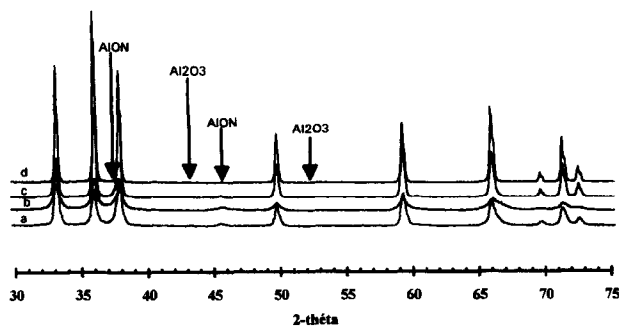


Fig. 4. XRD patterns of different AlN powders (a: 1400°C, b: 1500°C, c: 1600°C, d: 1800°C).

The heating occurs under a secondary vacuum with a rise of  $30^{\circ}\text{C min}^{-1}$  up to  $250^{\circ}\text{C}$ . The detection of the TL signals is achieved with a 'Hamamatsu R562' photomultiplier and an 'Oriel 50560' filter (0.1% of transmission). The signal is amplified with a 'Keithley 414S' picoamperemeter. The temperature and intensity of signal are measured every 2 s.

#### 2.4 Other techniques

Aluminium nitride powders were characterised by infrared spectroscopy (IR : Perkin-Elmer Model 1310 and Bomem), X-ray diffraction (Philips CGR Sigma 2070 and Siemens D500; quartz-filtered  $\text{CuK}\beta$  radiation) and microanalyser C-H-N (Carlo-Erba Model 1106).

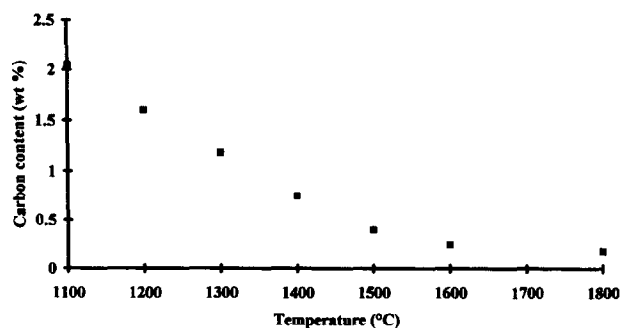


Fig. 5. Carbon content evolution versus of the temperature.

$^{27}\text{Al}$  NMR spectra were obtained using the Magic Angle Sample Spinning (MAS) technique using a Brüker DPX 400 at a resonance frequency of 104.26 MHz. The impulse at  $90^{\circ}$  was  $6 \mu\text{s}$ , the repetition time between two scans about 2 s. Four hundred scans were conducted with several spinning speeds: 0, 3, 5 and 8 kHz.

### 3 Results and Discussions

#### 3.1 Part A

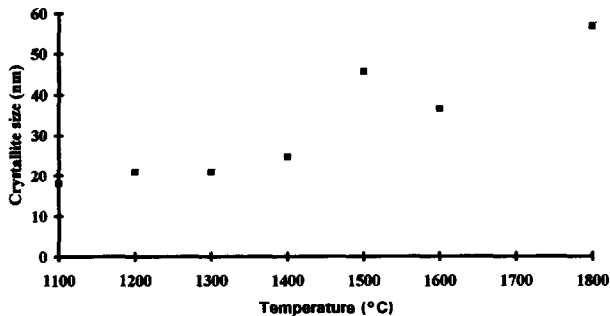
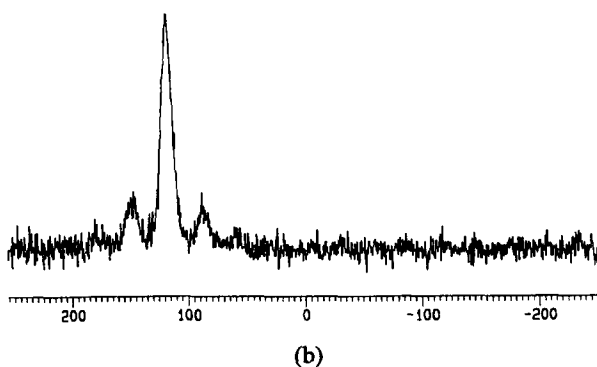
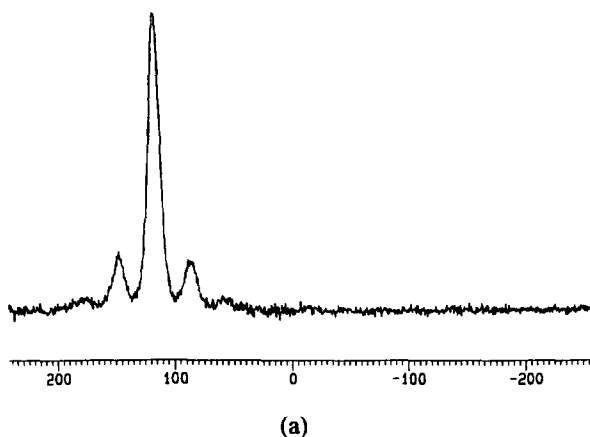
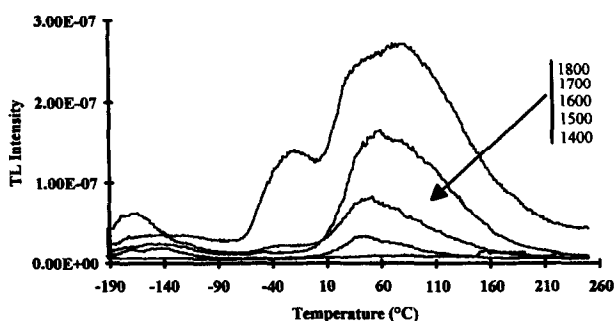
The pyrolysis of synthesis products at  $1100^{\circ}\text{C}$ . under ammonia flow ended with some amorphous powders. The FTIR pattern shows a broad strip at  $700 \text{ cm}^{-1}$  characteristic of AlN.<sup>23</sup> As a consequence, some thermal treatments were required in order to crystallise the powders.

Figure 4 shows the XRD patterns of the products. We observed the crystallisation of several phases after a 2H-würtzite-type compound identified to AlN and two oxide phases  $\gamma\text{-AlON}$  and  $\alpha\text{-Al}_2\text{O}_3$  phases crystallise from  $1100^{\circ}\text{C}$  and their volume reduces beyond  $1500^{\circ}\text{C}$ . The decrease of carbon content (Fig. 5) during the rise allowed us to suppose that a carboreduction mechanism was responsible for the missing oxide phases.

Lattice parameters of aluminium nitride were refined as (a)= $3.1141 \text{ \AA}$  and (c)= $4.9825 \text{ \AA}$  at  $1800^{\circ}\text{C}$  (Table. 1) These values were identical with those reported for AlN.<sup>2</sup> Accordingly,  $\text{Al}_2\text{OC}$ , which is an Al-containing isostructural compound with large lattice parameters (a= $3.19 \text{ \AA}$  and c= $5.09 \text{ \AA}$  and which forms some solid solutions with AlN<sup>9</sup> may be present in the 2H-würtzite-type compound in very small amounts. Hence, any carbon detected should be present as an amorphous phase. On the other hand, the observed lattice parameters of AlN (Table 1) suggest that the oxygen content is very small and decreases as a function of the temperature. Furthermore, crystallites size calculated with the FWHM, increases from 16 nm to 56 nm between  $1100^{\circ}$  and  $1800^{\circ}\text{C}$  (Fig. 6).

**Table 1.** Lattice parameters of different AlN powders

	1400°C	1500°C	1600°C	1800°C	AlN th
a (Å)	3.1096	3.1121	3.1150	3.1141	3.1105
c (Å)	4.9775	4.9804	4.9836	4.9825	4.9788

**Fig. 6.** Crystallite size evolution versus the temperature.**Fig. 7.**  $^{27}\text{Al}$  MAS NMR spectra of various AlN powder (a): AlN from our process and (b) : ATOCHEM Grade A-100T).**Fig. 8.** TL curves of different powders.

$^{27}\text{Al}$  NMR spectra were used to characterise the local first and second co-ordination spheres of aluminium atoms. Two samples were analysed\* (Fig. 7) : (a) AlN synthesised with our own process and treated for 3 h at 1800°C and (b) AlN Atochem Grade A2. Figure 7(a) shows one signal at a position of 118 ppm, other peaks were attributed to spinning sidebands. In fact, different authors<sup>24,25</sup> give  $^{27}\text{Al}$  shift of the  $\text{AlN}_4$  tetrahedra in AlN between 114 and 117 ppm; and  $\text{AlN}_4$  peaks in AlON at 114 ppm.

The substitution of nitrogen atoms by oxygen in the AlN lattice formed some  $\text{AlO}_6$  and  $\text{AlO}_4$  units: their  $^{27}\text{Al}$  chemical shifts were, respectively, at 14 ppm in  $\alpha\text{-Al}_2\text{O}_3$  and  $\gamma\text{-AlON}$  and  $\text{AlO}_6$ ; and between 55 and 80 in  $\gamma\text{-AlON}$ . These results seem to indicate that no  $\text{AlO}_x$  ( $x = 4$  or 6) were present in the powder treated at 1800°C. Furthermore, the (a) spectra were consistent with that obtained for AlN Atochem (Fig. 7(b)), in which the oxygen content was about 1.1–1.5 wt%. These  $^{27}\text{Al}$  MAS NMR spectra validate results obtained with the XRD patterns concerning the small amount of oxygen in the powder treated at 1800°C.

Figure 8 shows thermoluminescence curves of different powders with a very good reproducibility of measurements. Powders treated between 1100° and 1800°C were analysed but only these treated above 1400°C presented some TL signals. We observed three main peaks located at -150, -30 and 60°C. In fact, the use of a deconvolution program proves it is possible to decompose this last peak into two TL peak: 30 and 80°C whereas Benabdesselam<sup>26</sup> found three peaks. He attributes the first two (-150 and -30°C) to  $\gamma\text{-AlON}$  and the others (60°C) to AlN.

When the temperature of the thermal treatment increased, we noticed a rise of intensities and area of peaks. Furthermore, the analysis of the main peak during the rise of the thermal treatment temperature revealed the increase of the maximum intensity temperature: we observed the growth of the peak at  $T = 80^\circ\text{C}$  at the expense of the peak located at  $T = 30^\circ\text{C}$ . As a consequence, the change of the thermal treatment temperature modified the amount of traps centres per defects-type and accordingly the oxygen content in the final powder.

XRD patterns have proved that the weight percentage of AlN increased with the rise of the temperature in spite of the probable presence of a small amount of  $\gamma\text{-AlON}$  (undetectable XRD content) in the powder treated at a temperature beyond 1600°C since we observed some TL signals

\*MAS NMR spectra were discovered at the University of Bordeaux, in CESAMO laboratory by Dr I. Pianet

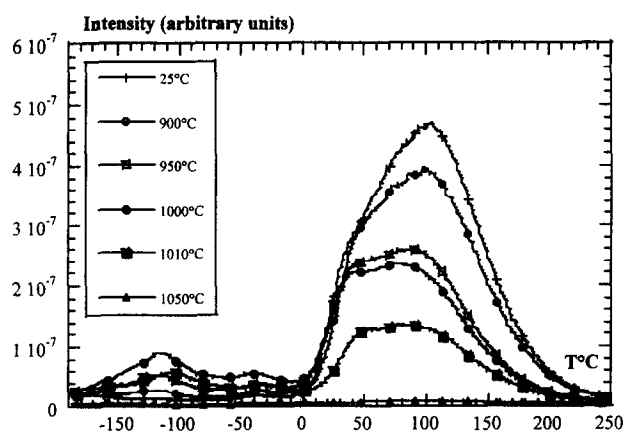


Fig. 9. Curves of thermoluminescence as a function of treatment temperature.

at  $-150$  and  $-30^{\circ}\text{C}$ . Nevertheless, we can conclude that the oxygen content decreased between  $1100$  and  $1800^{\circ}\text{C}$  by virtue of the absence of oxide phases and the increase of AlN lattice parameters. As a consequence, the presence of defects concentration is not solely responsible for the intensity of TL peaks. The light emission may be due to the crystallite size evolution. This well-known mechanism has already been observed in zirconia by Orleans<sup>27</sup> showed that crystallite and grain size influence TL curves.

### 3.2 Part B

Different treatments in oxygen for 3 h are achieved for temperatures between  $200$  and  $1100^{\circ}\text{C}$ . The obtained data curves are shown in Fig. 9. There is little variation in the thermoluminescence peaks until  $850^{\circ}\text{C}$ . However, following that, the intensity decreases sharply, nearly vanishing at  $1050^{\circ}\text{C}$ . In parallel, there is an appearance of peaks at low temperatures.

In fact, after  $900^{\circ}\text{C}$ , the thermal treatment of AlN modifies the intensity of the measured signal. An X-ray diffraction analysis of different powders

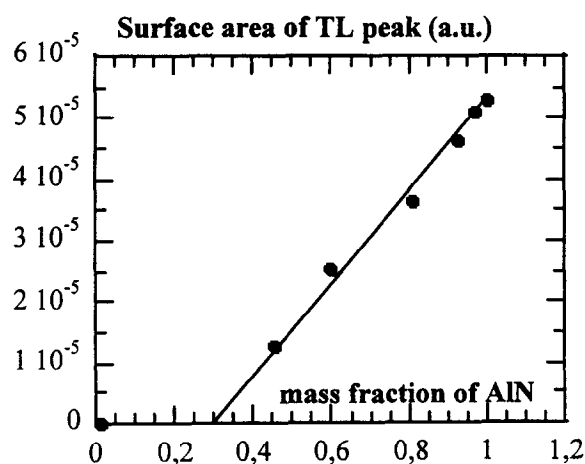


Fig. 10. Evolution of the intensity of TL signal as a function of AlN mass fraction.

allows the appearance of  $\theta\text{-Al}_2\text{O}_3$ , then  $\alpha\text{-Al}_2\text{O}_3$ . The recorded thermoluminescence variations indicate an evolution of the powder composition. It is noted that  $\theta\text{-Al}_2\text{O}_3$  is the better crystallized transition phase, others may be present, but are not detectable with this method.

After  $900^{\circ}\text{C}$ , peaks at low temperatures appear. Their intensity reaches a maximum at  $1000^{\circ}\text{C}$ , then diminishes to nearly vanish at  $1050^{\circ}\text{C}$ . This is characteristic of an intermediate species. It resembles that of  $\gamma\text{-AlON}$ , which has a thermoluminescence peak at the same temperature.<sup>26</sup> The IR spectrometry is used for confirmation.

The area of the principal peak as well as the nitride mass fraction varies as a function of the temperature of the thermal treatment. (The proportion of aluminium nitride in the powder is determined by weight before and after treatment, knowing that the total oxidation of AlN into alumina is accompanied by an increase in relative weight of 24%.) Also, there is a linear relation between the two factors (Fig. 10).

Consequently, the diminishment of the area of the peak at  $1000^{\circ}\text{C}$  is directly linked with the progressive disappearance of aluminium nitride to the benefit of alumina. The preceding line does not pass through the origin of the axes (Fig. 10). This could result from a phenomenon of limiting thickness. The layer of alumina forms at the surface of the grains. When the alumina reaches a critical thickness of  $0.2\ \mu\text{m}$ , it hinders the thermoluminescence signal from the AlN which remains at the core of the grain. Either the AlN does not further receive any UV radiation, or the emitted photons cannot cross the alumina barrier.

## 4 Conclusions

The reaction of aluminium iodide with propylamine, followed by the pyrolysis at  $1100^{\circ}\text{C}$  under ammonia flow and thermal treatments under nitrogen stream between  $1100^{\circ}$  and  $1800^{\circ}\text{C}$  ends at AlN-würtzite-structure in which impurities slipped into the lattice.

We have used several techniques in order to characterise final powders and to understand mechanisms. Among these, we have employed an original experiment well-suited to the analysis of aluminium nitride.

First XRD, patterns allow us to estimate the evolution of oxygen content in different powders, as oxide phases and substitution in the AlN lattice. <sup>27</sup>Al MAS NMR spectra of AlN treated at  $1800^{\circ}\text{C}$  showed the near absence of oxygen in the powder since no  $\text{AlO}_6$  and  $\text{AlO}_4$  units were observed (analysis of 97% atoms of <sup>27</sup>Al).

Finally, TL spectra have revealed another characteristic of AlN powder: their thermoluminescence is linked to the oxygen content but also to the crystallite size.

In contrast, we haven't manage to identify the nature of defects. Furthermore, the TL curve obtained at 1800°C presents a peak at -30°C with a higher intensity : it will be very interesting to study this powder with the spectral repetition of the main TL peaks to attribute more easily each band to each defect-type and to understand the surprising growth of this peak located at T= 30°C.

Besides, some additional experiments should be attempted in TL to determine the kinetic order, the frequency factor and the depth of traps with the Hoogenstraaten method (parameters characteristic of a TL signal).

Concerning the behavior of AlN Pyrofine R in oxygen between 200 and 1100°C, a correlation between diminishing thermoluminescence signal and progressive oxidation of aluminium nitride is presented, with evidence, for the temperature between 800 and 1000°C.

## References

- Billy, M., Labbe, J. C., Lee, Y. M. and Roullet, G., Résistance du nitrure d'aluminium à l'irradiation par neutrons rapides. *Rev. Int. Hautes Tempér. Réfract. Fr.*, 1984, **21**, 19-25.
- Slack, G. A. and Bartram, S. F., Thermal expansion of some diamondlike crystals. *J. Appl. Phys.*, 1975, **46**, 89-98.
- Berger, A., Inversion domains in aluminium nitride. *J. Am. Ceram. Soc.*, 1991, **74**, 1148-1151.
- Solanki, A. K., Kashyap, A., Nautiyal, T. and Auluck, S., Optical properties of AlN. *Solid State Communications*, 1995, **94**, 1009-1012.
- Mullot, J., Lecompte, J. P. and Jarrige, J. High thermal conductivity aluminium nitride substrates prepared by tape casting with Y2O3 or YF3 additives. In *Proceedings of the Fourth International Conference of the European Ceramic Society Part II*, ed. C. Galassi. Gruppo Editoriale Faenza Editrice S. p. A., 1995, pp. 235-241.
- Kuromitsu, Y., Yoshida, H., Ohno, S., Masuda, H., Takebe, H. and Morinaga, K., Oxidation of sintered aluminium nitride by oxygen and water vapor. *J. Ceram. Soc. of Jpn.*, 1992, **100**, 70-74.
- Bowen, P., Highfield, J. G., Mocellin, A. and Ring, T. A., Degradation of aluminium nitride powder in an aqueous environment. *J. Am. Ceram. Soc.*, 1990, **73**, 724-728.
- Kurokawa, Y., Utsumi, K. and Takamizawa, H., Development and microstructural characterization of high-thermal conductivity aluminium nitride ceramics. *J. Am. Ceram. Soc.*, 1988, **71**, 588-594.
- Slack, G. A., Non-metallic crystals with high thermal conductivity. *J. Phys. Chem. Solids*, 1973, **34**, 321-335.
- Harris, J. H., Youngman, R. A. and Teller, R. G., On the nature of the oxygen-related defect in aluminium nitride. *J. Mater. Res.*, 1990, **5**, 1763-1772.
- Lecompte, J. P. Contribution à l'étude de frittage sous charge du nitrure d'aluminium. Thèse de Doctorat, Laboratoire de Céramiques Nouvelles, Limoges 1982.
- Archangelskii, G. E., Karel, F., Mares, J., Pacesova, S. and Pastrnak, J., The luminescence and EPR spectra of manganese activated AlN. *Phys. Stat. Sol. (a)*, 1982, **69**, 173-183.
- Baltramiejunas, R., Vaitkus, J., Narkeircius, V., Niunka, V., Mares, J. and Pastrnak, J., Luminescence of Aln at high excitation levels with or without Mn and Eu doping. *Sovi. Phys. Coll.*, 1975, **15**, 64-68.
- Karel, F., Pastrnak, J., Hejduk, J. and Losik, V., Fine structure of emission spectra of the red AlN:Mn luminescence. *Phys. stat. sol.*, 1966, **15**, 693-699.
- Karel, F. and Mares, J., Electron states of manganese luminescence centres in AlN. *Czech. J. Phys. B.*, 1972, **22**, 847-853.
- Harris, J. H. and Youngman, R. A., Time-resolved luminescence of oxygen related defects in aluminium nitride. *Mat. Res. Soc. Symp. Proc.*, 1990, **167**, 253-258.
- Rosa, J., Mechanism of thermoluminescence in AlN:O. *Czech. J. Phys. B.*, 1979, **29**, 810-824.
- Pastrnak, J., Pacesova, S. and Roskovcova, L., Luminescent properties of the oxygen impurity centres in AlN. *Czech. J. Phys. B.*, 1974, **24**, 1149-1161.
- Pastrnak, J., Hejda, B., Kubatova, J., Malek, J. and Pacesova, S., Deep energy levels in aluminium nitride : calculations and optical and transport measurements. In *Proceedings of the 13th International Conference Physical Semiconductor*, Rome, 1976, pp. 591-594.
- Pacesova, S. and Jastrabik, L., The energy spectrum of a deep impurity—Oxygen in AlN. *Phys. Stat. Sol. (b)*, 1979, **93**, K111-14.
- Pastrnak, J., Pacesova, S., Sanda, J. and Rosa, J., Luminescence of oxygen centres in AlN. *Izvestiya Akademii Nauk SSSR. Seriya Fizicheskaya*, 1973, **37**, 599-602.
- Porte, F., Lecompte, J. P., Tétard, D. and Jarrige, J. Aluminium nitride synthesis with aluminium halides and ammonia or amines. In *Proceedings of the Fourth International Conference of the European Ceramic Society Part I*, ed. C. Galassi. Gruppo Editoriale Faenza Editrice S.p.A., 1995, pp. 45-52.
- Sappei, J., Goeuriot, D., Thevenot, F., Laurent, Y., Guyader, J. and L'Haridon, P., Alumina- $\gamma$ -aluminium oxynitride composites from alumina nitrated by ammonia. *J. Europ. Ceram. Soc.*, 1991, **8**, 257-262.
- Hayashi, S., Hayamizu, K. and Yamamoto, O., <sup>27</sup>Al High-resolution solid-state NMR study of hydration of ultrafine powder of aluminium nitride. *Bull. Chem. Soc. Jpn.*, 1987, **60**, 761-762.
- Fitzgerald, J. J., Kohl, S. C. and Piedra, G., Observation of four-coordinate aluminium oxynitride (AlO<sub>4-x</sub>N<sub>x</sub>) environments in ALON solids by MAS <sup>27</sup>Al NMR at 14 T. *Chem. Mater.*, 1994, **6**, 1915-1917.
- Benabdesselam, M., Iacconi, P., Lapraz, D., Grosseau, P. and Guilhot, B., Thermoluminescence of AlN. Influence of synthesis processes. *J. Phys. Chem.*, 99, 1995, 10319-10223
- Orlans, P., Etude physicochimique des oxydes de zirconium et du dispersoide alumine-zircone. Thèse de Doctorat, Institut National Polytechnique de Grenoble & Ecole Nationale Supérieure des Mines de Saint-Etienne, Saint-Etienne, 1987.